2013 American Control Conference (ACC)
Washington, DC, USA, June 17-19, 2013

Response time re-scaling and Weber's law in adapting biological systems

Abdullah Hamadeh*,†, Eduardo Sontag†, Brian Ingalls*,‡

***Abstract*— Systems biology has revealed numerous examples of networks whose dynamic behavior is robust to system perturbations and noise. In many cases, this behavior arises from simple yet fundamental features of the system architecture. A well-studied example is the chemotactic response of *Escherichia coli*. In various models of this system, it is shown that simple assumptions on the receptor methylation dynamics lead to robust perfect adaptation of chemotactic activity.**

Recent experimental work has also shown that the transient *E. coli* chemotactic response is unchanged by a scaling of its ligand input signal; this behavior is called *fold change detection* (FCD), and is in agreement with earlier mathematical predictions. However, this prediction was based on very particular assumptions on the structure of the chemotaxis pathway. In this work, we begin by showing that behavior similar to FCD can be obtained under weaker conditions on the system structure. Namely, we show that under relaxed conditions, a scaling of the chemotaxis system's inputs leads to a time scaling of the output response. We propose that this may be a contributing factor to the robustness of the experimentally observed FCD. We further show that FCD is a special case of this time scaling behavior for which the time scaling factor of unity.

We then proceed to extend the conditions for output time scaling to more general adapting systems, and demonstrate this time scaling behavior on a published model of the chemotaxis pathway of the bacterium *Rhodobacter sphaeroides*. This work therefore provides examples of how robust biological behavior can arise from simple yet realistic conditions on the underlying system structure.

I. Introduction

Signal processing and control mechanisms of a remarkable level of sophistication have been revealed to be at the heart of many cellular processes. The capability of cells to extract and process information from their environment allows them to optimize their responses and their allocation of resources, thus bequeathing selective advantages to the organism. However, such an ability must necessarily be a robust property for it to be effective in the cell's noisy and uncertain environment. A key aim of systems biology is to identify the mechanisms through which robustness is achieved in cellular processes.

Such sources of robustness can be identified through the analysis of models of biological systems. An example of this is adaptation in the *Escherichia coli* chemotaxis model. In [1] it was shown that adaptation of chemotactic activity in the model presented in [2] can be explained as an instance of integral feedback control. Two simple biochemical assumptions are sufficient for this mechanism to arise, namely that the enzyme CheR methylates only inactive receptors, whilst CheB demethylates only active receptors. Moreover, as a consequence of integral control, adaptation in this system is a property that is robust to variations in biochemical parameters such as protein copy numbers and rates of methylation and phosphorylation reactions.

In a further, more recent, study of bacterial chemotaxis response [3], it was shown that the dynamic model of the chemotaxis system presented in [4] displays a property known as Fold Change Detection (FCD). With this property, the chemotaxis output response is invariant under scalings of its sensed ligand input, as illustrated in Figure 1. This depends on two assumptions on the chemotaxis system. The first is that the system shows logarithmic tracking of its sensed ligand input. The second assumption is that the average receptor activity is a sigmoidal function of the average receptor methylation state at a fixed ligand level.

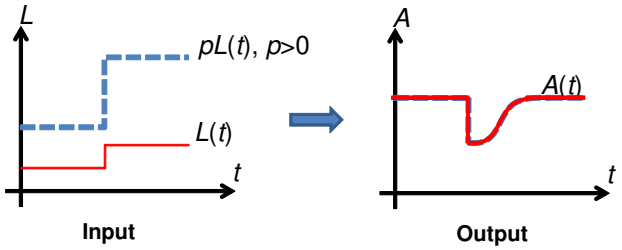

Fig. 1. Fold change detection: a scaling of the input signal $L(t)$ has no effect on the adapting output $A(t)$.

In this work, we show that with some simple conditions on the structure of adapting systems, qualitative behavior that approximates FCD can be observed. In particular, we show that in response to step inputs, these conditions lead to the feature that the maximum amplitude of the output response is invariant under a scaling of the input, a property known as Weber's law [8], illustrated in Figure 2. To demonstrate this, we give conditions under which a scaling of a step input will lead to an output response that is a time scaled version of the system's response to an unscaled input. We also show that these conditions on system structure are less restrictive than those required for FCD, which is what would be expected from the fact that Weber's law is a weaker property than FCD.

This paper is organized as follows: we first give a brief introduction to the *E. coli* chemotaxis network and review the properties of this system that lead to FCD. We then show that by relaxing some of the conditions on the model structure the system will no longer exhibit FCD, but it will display the weaker property of Weber's law. After presenting conditions for this property in more general systems, we demonstrate our results on the more complex chemotaxis model of the bacterium *Rhodobacter sphaeroides*.

* Department of Applied Mathematics, University of Waterloo, Waterloo, Ontario, Canada. Email: bingalls@uwaterloo.ca (Brian Ingalls)

†Department of Mathematics, Rutgers University, Piscataway, New Jersey, USA. Emails: abdullah.hamadeh@rutgers.edu (Abdullah Hamadeh) sontag@math.rutgers.edu (Eduardo Sontag)

‡Corresponding author

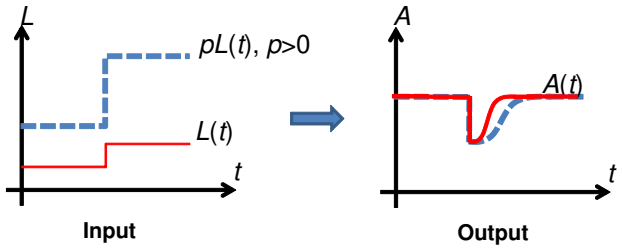

Fig. 2. Weber's law: a scaling of the input $L(t)$ leads only to a time scaling of the adapting output $A(t)$.

With this work, we aim to further the idea that robust biological behavior arises from simple conditions that are relatively insensitive to parameter values. We believe that this approach to understanding the dynamics of biological systems can provide insight into how cellular modules interact to produce structured behavior, and can offer some ideas on how robust synthetic circuits can be designed.

II. Properties of the *E. coli* Chemotaxis System Output Response

A. A review of adaptation in E. coli chemotaxis

Many bacteria have evolved *chemotaxis* mechanisms with which to navigate their environment towards chemically favorable conditions. In the bacterium *E. coli* this is achieved through a biochemical feedback system that controls its random walk pattern of swimming by modifying the activity of the molecular 'brake' that acts on the bacterium's propulsive flagella [2], [6]. As shown in Figure 3 protein receptors (known as methyl-accepting chemotaxis proteins) span the bacterial cell's membrane, detect ligands in the cell's environment, and undergo methylation and de-methylation reactions in the cell's interior. Methylation of the receptors increases their activity in triggering the phosphorylation of a chain of chemotaxis signalling proteins. Activation of this cascade culminates in the phosphorylation and activation of the protein CheY, which interacts with the bacterium's flagella, causing an increase in the frequency of stopping and re-orientation of the cell. In contrast, a sensed increase in chemoattractant ligands causes this activity to fall, resulting in smooth swimming. At the same time, phosphorylation of the chemotaxis protein cascade results in the activation of the chemotaxis protein CheB, which increases the de-methylation rate of the receptors. Thus, a sensed increase in the ligand concentration causes the activity level to fall, increasing the average swim length, but this is followed by a decrease in the de-methylation rate of the receptors. The subsequent increase in methylation restores the activity, and hence the average swim length, to its pre-stimulus level. This return to the same average swim length, a feature termed *adaptation*, is observed over a wide ligand concentration range. The source of this adaptation can be traced to the specificity with which the chemotaxis proteins bind and methylate and de-methylate receptors, a process that takes place on a slower time scale than the activation of the protein cascade [6]. The protein CheR, which operates at saturation, preferentially methylates receptors that are inactive, whereas the protein CheB is known to preferentially de-methylate active receptors [1]. Denoting the average methylation level of receptors by m and the activity level as a, after a quasi-steady state assumption on the phosphorylation dynamics, the methylation dynamics can be approximated by

$$\dot{m} = R(a)(1-a) - B(a)a, \quad a = G(m, L) \tag{1}$$

where $R(a)$ quantifies the rate of methylation of inactive receptors and is increasing in a, $B(a)$ represents the rate of de-methylation of active receptors and is also increasing in a, and L is the ligand concentration level. More generally however, and for the purposes of our analysis, the methylation dynamics can be represented, as in [4], as

$$\dot{m} = F(a), \quad a = G(m, L) \tag{2}$$

where $F(a)$ is a continuous, strictly monotonically decreasing function of a and G is a continuous function where $\frac{\partial G}{\partial m} > 0$, $\frac{\partial G}{\partial L} < 0$ (due to the effects of methylation and ligand binding in respectively increasing and decreasing receptor activity). Note that with this structure, system (2) exhibits adaptation: it has a unique fixed point for any L, and the output at any fixed point, given by $a = F^{-1}(0)$, is independent of L. Thus, relatively mild monotonicity conditions lead to a robust adaptation behavior regardless of the exact values of this system's parameters [2], [1]. In this paper, we argue that further qualitative and robust dynamic behaviors can also be obtained from simple conditions on system structure. In particular, we show that similar monotonicity conditions can be sufficient for adapting systems such as the *E. coli* chemotaxis system to exhibit Weber's law [8].

Many variations of the model (1) exist, including that in [7] where the dependence of B on a is assumed to be dynamic and where the methylation dynamics are not averaged, but split into a series of ODEs that model the varying degrees of methylation of the receptors.

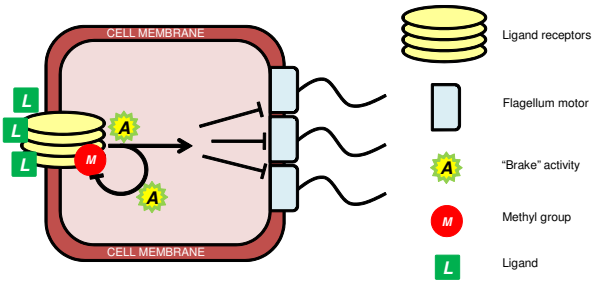

Fig. 3. Schematic of the *E. coli* chemotaxis pathway.

B. Models of E. coli chemotactic activity

The chemotaxis model in [4] is of the form in (2). It departs from previous models such as [2], [7] in its use of a thermodynamic approach to construct a model of the average receptor activity as a function of the average methylation level m and the sensed ligand concentration L, based on the Monod-Changeaux-Wyman allosteric model [9]. The form given for the activity in that reference is

$$a(m,L) = \frac{1}{1+\exp(f_t)} \tag{3}$$

where

$$f_t = N(f_m(m) + f_L(L)) \tag{4}$$

with N being the size of receptor clusters and $f_m(m)$, $f_L(L)$ being the contributions to the free energy difference between active and inactive receptors due to methylation and ligand binding respectively. It is shown in [10], [4] that $f_L(L) = \ln(1+\frac{L}{K_I}) - \ln(1+\frac{L}{K_A})$, where the logarithmic form comes from the change in ligand translational entropy due to receptor binding. In [4], [11] it is shown by data fitting that $f_m(m)$ is an approximately affine, decreasing function of m and is given by $f_m(m) = \alpha(m_0 - m)$. In the range of ligand concentrations $K_I \ll L \ll K_A$, the system (3), (4) can be approximated by

$$a(m,L) = \frac{1}{1+\exp[N(\alpha(m_0-m))]\left[\frac{L}{K_I}\right]^N} \tag{5}$$

We can alternatively use mass action kinetics to arrive at a model for the activity given by

$$a(m,L) = \frac{1}{1+\frac{1}{h(m)}\left[\frac{1+\frac{L}{K_I}}{1+\frac{L}{K_A}}\right]^N} \tag{6}$$

(see Appendix) which is of a form very similar to that in [4]. Note also that in the ligand range $K_I \ll L \ll K_A$ we can make an approximation of (6) that is similar to (5):

$$a(m,L) = \frac{1}{1+\frac{1}{h(m)}\left[\frac{L}{K_I}\right]^N} \tag{7}$$

As discussed in the Appendix, the function $h(m)$ quantifies the ratio of active to inactive receptors when $L = 0$. We assume that $h(m)$ is strictly increasing based on the fact that the kinase activity of the receptor complex increases with the average receptor level of methylation. We further assume that $h(m)$ is differentiable. Note that using the alternative modeling approach of [4], the ratio of active to inactive receptors when $L = 0$ is given by $\frac{a(m,0)}{1-a(m,0)} = e^{N\alpha(m-m_0)}$ which, as with $h(m)$, is an increasing function of m.

Reference [5] presents the activity level $A_M(L)$ of a receptor in the M^{th} methylation state (where $M \in \{0,1,2,3,4\}$) when the ligand concentration is L by

$$A_M(L) = \frac{1}{1+\frac{1-p_M}{p_M}\frac{1+\frac{L}{K_I}}{1+\frac{L}{K_A}}} \tag{8}$$

where p_M is the probability of activity of a receptor in the M^{th} methylation state when $L = 0$. From [12], these probabilities are $p_0 = 0$, $p_1 = 0.125$, $p_2 = 0.5$, $p_3 = 0.874$ and $p_4 = 0.997$. By fitting a continuous function of the average methylation level m to $A_M(0)$, we can arrive at a model of the form (6). With the above values of $p_0, \cdots, p_4$, the model $A_M(0)$ can be approximated by the Hill function $a(m,0) = \frac{m^4}{m^4+15}$ (see Figure 4). At the ligand level L,

$$a(m,L) = \frac{1}{1+\frac{15}{m^4}\left[\frac{1+\frac{L}{K_I}}{1+\frac{L}{K_A}}\right]} \tag{9}$$

Note that here, $h(m) = \frac{m^4}{15}$ and $N = 1$.

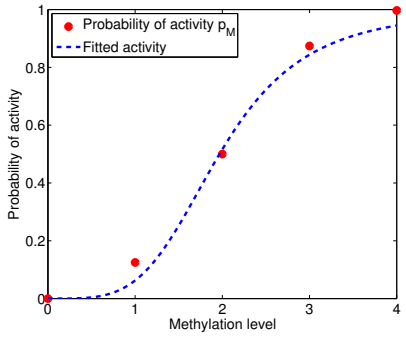

Fig. 4. The average chemotaxis receptor activity in *E. coli* is an increasing function of the average receptor degree of methylation. Shown here is a fit of the average activity level $a(m,0)$ to the probabilities of activity p_M which are estimated in [12]) for different average methylation levels.

In the following section we will be making use of the following approximation to the receptor activity: in the range $K_I \ll L \ll K_A$, (9) can be approximated by

$$a(m,L) \approx \frac{1}{1+\frac{15}{m^k}\left[\frac{L}{K_I}\right]} \tag{10}$$

C. FCD and Weber's law in the E. coli chemotactic response

In agreement with theoretical predictions made in [3] based on the model (2), (5), it was experimentally shown in [13] that *E. coli* displays *fold change detection* (or, FCD) in its activity in the ligand range $K_I \ll L \ll K_A$. This is the property, illustrated in Figure 1, that the chemotaxis system output activity $a(t)$, in response to ligand inputs $L(t)$ and $pL(t)$, $p > 0$ are identical when the initial conditions are the steady states pre-adapted to the constant inputs $L(0)$ and $pL(0)$ respectively. More formally, if (2), (5) exhibits a solution $m_1(t)$ in response to an input ligand signal $L_1(t)$ (with initial condition pre-adapted to the constant input $L_1(0)$), and a solution $m_2(t)$ in response to an input ligand signal $L_2(t) = pL_1(t)$, $p > 0$ (with initial condition pre-adapted to the constant input $L_2(0) = pL_1(0)$), then the outputs $a_1(m_1(t), L_1(t))$, $a_2(m_2(t), L_2(t))$ resulting from the two solutions are such that $a_1(t) = a_2(t)$.

We shall next show that, in response to step inputs, output behavior similar to FCD can be achieved by model (2), (9) in the ligand range $K_I \ll L \ll K_A$, where (10) holds. Consider the model (2), (10), subject to a step input $L(t)$ (where, without loss of generality, the step is taken at time $t = 0$), and assume that the initial state is pre-adapted to the constant input $L(0)$. We denote the solution in response to this input by $m(t) = \phi(t)$ and the corresponding output $a(\phi(t), L(t))$. Now suppose that the input is scaled by a factor $p > 0$. Adopting the change of variable $w^4 = m^4 p^{-1}$, the chemotaxis system (2), (10) can be written as

$$\frac{dw}{dt} = p^{-\frac{1}{4}} F(a), \quad a(w,L) = \frac{1}{1+\frac{15}{w^4}\left[\frac{L}{K_I}\right]} \tag{11}$$

Defining time scale $T = p^{-\frac{1}{4}}t$, we can re-write (11) as

$$\frac{dw}{dT} = F(a), \quad a(w,L) = \frac{1}{1+\frac{15}{w^4}\left[\frac{L}{K_I}\right]} \tag{12}$$

Now since the input signal is a step input at time $t = T = 0$, it follows that $L(T) = L(t)$. In the new time scale (12) is identical to the original system (2), (10) and therefore $w(T) = \phi(T) = \phi(p^{-\frac{1}{4}}t)$. The resulting activity is then $a(\phi(T), L(T))$, a time scaled version of the output resulting from the unscaled input $L(t)$. Figure 5 (left) shows the simulations of the model (1), (10) where $K_I = 18$, $k_r = k_b = 1$, subject to three step inputs scaled by $p = 1, 5, 10$. The right panel shows that time scaling the outputs by $p^{\frac{1}{4}}$ aligns them, demonstrating that scaling the input by p causes a time scaling of the output by $p^{-\frac{1}{4}}$, as shown above.

Weber's law is the property whereby systems exhibit the same maximal output in response to a given proportional change in input. As shown in Figure 2, the time scaling behavior shown here is an example of Weber's law, since, by definition, a mere time scaling of the adapting output will leave its maximum amplitude unchanged, but will cause a stretching of the response along the time axis. In Section III we will show that the only condition needed on $h(m)$ for such time scaling behavior to hold in response to step inputs is strict monotonicity. Therefore as with adaptation, we find that a monotonicity condition is sufficient to yield a robust dynamic property: $F(a)$ being strictly monotonically decreasing leads to adaptation, whilst $h(m)$ being strictly monotonic leads to Weber's law.

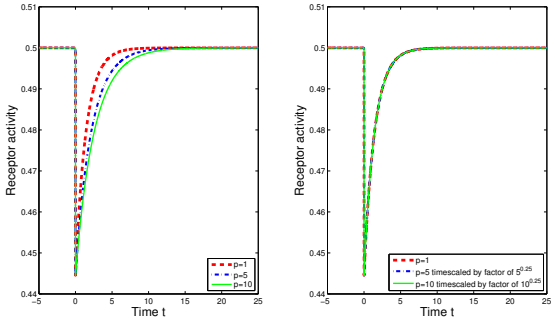

Fig. 5. Left: Simulated outputs $a(t)$ of the model (2), (10) subject to inputs $pL(t)$, $p = 1, 5, 10$. The signal $L(t)$ is a 25% step at time $t = 0$, where $L(0_-) = 75$. Right: Simulated outputs time scaled by $p^{\frac{1}{4}}$.

If instead of $h(m) = \frac{m^4}{15}$ we have $h(m) = e^{\alpha(m-m_0)}$ as in [4], repeating the analysis above (with the change of variable $e^{\alpha w} = e^{\alpha m}p^{-1}$) yields $T = t$, a time scaling factor of unity. Therefore scaling the input $L(t)$ by $p > 0$ yields the same output $a(t)$, which is fold change detection as defined by [3], [13], [14].

III. Results

In the following we will be studying how the output response of dynamical systems of the form

$$\begin{aligned} \frac{dx}{dt}(t) &= f(x(t), u(t), y(t)), \quad x \in X \subset \mathbb{R}^n, u \in \mathbb{R} \\ y(t) &= g(x(t), u(t)) \quad y \in \mathbb{R}^q \end{aligned} \tag{13}$$

changes under transformations of the input signal $u(t)$. We will assume that (13) has a unique steady state $\sigma(u)$ for each constant input u.

Definition 1 (Response time re-scaling): Consider a class of input signals $\mathcal{U}$ and a class of transitive and surjective input transformations Π, where $\pi \in \Pi$ is such that $\pi : \mathbb{R} \mapsto \mathbb{R}$. System (13) exhibits response time re-scaling (RTR) with respect to inputs $u \in \mathcal{U}$ and input transformations Π if $\forall u \in \mathcal{U}$ and $\forall \pi \in \Pi$ there exists $T = T(t)$, $T \in \mathcal{K}_\infty$ such that $g(x(t), u(t)) = g(x(T(t)), \pi(u(T(t))))$.

Proposition 1 presents a condition for (13) to display RTR in the sense of Definition 1 when it is subject to inputs in the set $\mathcal{U}_s$, which we define as follows: $u(t) \in \mathcal{U}_s$ if

$$u(t) = \begin{cases} \mu_0 & t = 0 \\ \mu & t > 0 \end{cases}$$

for any constants $\mu, \mu_0 > 0$.

Proposition 1: Consider (13) subject to input $u \in \mathcal{U}_s$ and with initial state $\sigma(u(0))$. Suppose that for all π in the class of transitive and surjective input transformations Π there exist $\rho : X \mapsto X$, $\lambda : X \mapsto \mathbb{R}_{>0}$ which are such that

$$\begin{aligned} \rho_*(x) f(x, \pi(u)) &= \lambda(\rho(x)) f(\rho(x), u) \\ g(x, \pi(u)) &= g(\rho(x), u) \end{aligned} \tag{14}$$

where ρ_* denotes the Jacobian of ρ. Then system (13) exhibits response time re-scaling in the sense of Definition 1 with $T^{-1}(t) = \int \lambda(\rho(x(t)))\, dt$, $T(0) = 0$.

Proof: Let $u \in \mathcal{U}_s$ and denote by $x(t) = \phi(t, \sigma(\pi(u(0))), \pi(u))$ the solution to (13) with input $\pi(u)$ and with initial state $\sigma(\pi(u(0)))$, yielding output

$$y(t) = g(x(t), \pi(u(t))) \tag{15}$$

Note that by the surjectivity of π we have $\pi(u) \in \mathcal{U}_s$.

Next, let $\theta(s) = \int \lambda(\rho(x(s)))\, ds$, $\theta(0) = 0$. Consider the signal $z(t) = \rho(x(\theta^{-1}(t)))$, which obeys

$$\frac{dz}{dt}(t) = \rho_*(x(\theta^{-1}(t))) f(x(\theta^{-1}(t)), \pi(u(\theta^{-1}(t)))) \frac{d\theta^{-1}(t)}{dt} \tag{16}$$

Observe that

$$\frac{d\theta^{-1}(t)}{dt} = \frac{1}{\theta'(\theta^{-1}(t))} = \frac{1}{\lambda(\rho(x(\theta^{-1}(t))))} = \frac{1}{\lambda(z(t))} \tag{17}$$

Using (14), (17) and the fact that $u(t) = u(\theta^{-1}(t))$, we obtain from (16) that

$$\frac{dz}{dt}(t) = \lambda(z(t)) f(z(t), u(t)) \frac{1}{\lambda(z(t))} = f(z(t), u(t))$$

which has solution $z(t) = \phi(t, \sigma(u(0)), u)$ and output $y(t) = g(z(t), u(t))$. From (14) and the relation $u(t) = u(\theta^{-1}(t))$, this output can be written as

$$y(t) = g(\rho(x(\theta^{-1}(t))), u(t)) = g(x(\theta^{-1}(t)), \pi(u(\theta^{-1}(t)))) \tag{18}$$

Comparing (15) and (18), we find that the output $y(t)$ arising from (13) subject to input $\pi(u)$ and with initial state $\sigma(\pi(u(0)))$ is equal to the output $y(t)$ arising from the input u and initial state $\sigma(u(0))$ when the former is time scaled by $\theta^{-1}(t)$. Therefore under step inputs u and $\pi(u)$, with $\pi \in \Pi$, and under the respective steady state initial conditions $\sigma(u(0))$ and $\sigma(\pi(u(0)))$, system (13) exhibits RTR in the sense of Definition 1 with $T = \theta^{-1}$. ■

A consequence of the transitivity of input transformations $\pi \in \Pi$ is that systems (13) exhibiting RTR also show adaptation in y, as demonstrated in the following corollary.

Corollary 1 (Adaptation): When at the steady state $\sigma(\mu_0)$, corresponding to a constant input μ_0, systems of the form (13) that show RTR in the sense of Definition 1 exhibit a constant output y that is independent of μ_0.

Proof: Denote by $x(t) = \phi(t, x(0), u)$ the solution to (13). When $u(0) = \mu_0$ and $x(0) = \sigma(\mu_0)$, the system exhibits output $y(0) = g(\phi(0, \sigma(\mu_0), \mu_0), \mu_0)$. Similarly, when $u(0) = \pi(\mu_0)$ for some $\pi \in \Pi$ and $x(0) = \sigma(\pi(\mu_0))$, the output is $y(0) = g(\phi(0, \sigma(\pi(\mu_0)), \pi(\mu_0)), \pi(\mu_0))$. Since the system exhibits RTR, we have that

$$g(\phi(0, \sigma(\mu_0), \mu_0), \mu_0) = g(\phi(0, \sigma(\pi(\mu_0)), \pi(\mu_0)), \pi(\mu_0))$$

Since π is transitive, it follows that for any pair of constants μ_0, ν_0, there exists π such that $\nu_0 = \pi(\mu_0)$. Therefore for any constants μ_0, ν_0, it follows that $g(\phi(0, \sigma(\mu_0), \mu_0), \mu_0) = g(\phi(0, \sigma(\nu_0), \nu_0), \nu_0)$, showing that steady state responses of systems (13) to constant inputs yield the same outputs y. ■

To compare the sufficient conditions for RTR with those for FCD under step inputs, note that the conditions given in [3] are identical to (14) except that the function $\lambda(\rho(\cdot))$ in Proposition 1 needs to be identically equal to one for FCD.

In Section II-C we observed that Weber's law can be observed in the response of *E. coli* chemotaxis models in the sense that a magnitude scaling of a step change in sensed ligand input leads to a time scaling of the observed chemotactic activity. This section has given conditions for response time re-scaling as per Definition 1. In its usual definition, Weber's law is defined as the conservation of the maximal amplitude of a system's output response after a positive scaling of its input signal [4]. It is a weaker property than RTR, with RTR implying Weber's law. This can be seen visually in the simple example in Figure 6. In the top panel, the two output responses display Weber's law but not RTR, since, although the two responses have the same maximal amplitude, it is clear that a mere time scaling will not align the two curves. In the bottom panel, the two responses show both Weber's law and RTR, since the two curves can be aligned by a sufficient horizontal scaling of either.

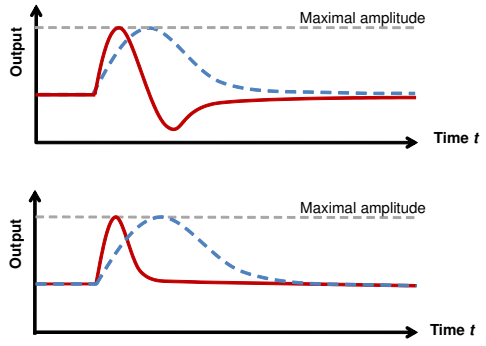

Fig. 6. Top: Weber's law response but not RTR. Bottom: Weber's law response and RTR.

A. RTR in response to multiplicative and additive input transformations

Integral feedback control is the feature of *E. coli* chemotaxis models such as [2], [4] that is responsible for adaptation. References [13], [3], [14] also give conditions under which such systems exhibit FCD. Here we consider two particular classes of integral feedback systems; the first shows RTR under multiplicative input transformations and the other shows RTR under additive transformations.

Proposition 2: Systems of the form

$$\begin{aligned} \dot{x} &= F(y) \quad x \in \mathbb{R}, u \in \mathbb{R}_{>0} \\ y &= G(h(x)u^r) \quad y \in \mathbb{R}, r \in \mathbb{R} \end{aligned} \tag{19}$$

where $h : \mathbb{R} \mapsto \mathbb{R}$ is an invertible, differentiable function, satisfy the conditions of Proposition 1 and hence exhibit RTR in the sense of Definition 1 under multiplicative transformations of the step input u, of the form $\pi(u) = pu$, $p > 0$.

Proof: Setting $\rho(x) = h^{-1}(h(x)p^r)$ and

$$\lambda(x) = \frac{p^r}{h'(x)} h' \left(h^{-1} \left(\frac{h(x)}{p^r} \right) \right)$$

we find that $G(h(x)u^r p^r) = G(h(\rho(x))u^r)$ and

$$\rho_*(x) F(G(h(x)u^r p^r)) = \lambda(\rho(x)) F(G(h(\rho(x))u^r))$$

Note that $\lambda(x) > 0$ since the invertibility of h guarantees that the ratio of $h' \left(h^{-1} \left(\frac{h(x)}{p^r} \right) \right)$ and $h'(x)$ is positive. The conditions of Proposition 1 for RTR are thus satisfied. ■

Corollary 2: Systems of the form

$$\begin{aligned} \dot{x} &= F(y) \quad x \in \mathbb{R}, v \in \mathbb{R}_{>0}, r \in \mathbb{R} \\ y &= G(k(x) + \gamma v) \quad y \in \mathbb{R}, \gamma \in \mathbb{R} \end{aligned} \tag{20}$$

where $h : \mathbb{R} \mapsto \mathbb{R}$ is an invertible, differentiable function, satisfy the conditions of Proposition 1 and exhibit RTR in the sense of Definition 1 in response to additive transformations of step input v, of the form $\pi(v) = v + p$, $p > 0$.

Proof: By defining $\tilde{G}(\cdot) = G(\ln(\cdot))$ we can re-write the output of (20) as $y = \tilde{G}(h(x)u^r p^r)$ where $h(x) = \exp(k(x))$, $u = \exp(v)$, $r = \gamma$. With these definitions, we can then directly apply Proposition 2 to system (20). ■

IV. Example

Unlike the *E. coli* chemotaxis network, that of the bacterium *Rhodobacter sphaeroides* has two distinct sensory clusters, one spanning the cell membrane that senses the presence of ligands in the bacterium's environment, and another within the cytoplasm that is believed to integrate internal metabolic information with the externally sensed ligand concentration signal [6]. These receptors control the kinase activity of chemotaxis proteins that phosphorylate a number of proteins analogous to the CheY and CheB proteins in *E. coli*. Two of these proteins, CheB_1, CheB_2, play a role analogous to CheB in *E. coli*, de-methylating the receptors. The *R. sphaeroides* chemotaxis model in [15] suggests that CheB_1 acts on the membrane cluster whilst CheB_2 de-methylates both clusters.

Two states, m_1 and m_2, represent the average methylation states of the membrane and cytoplasmic receptors respectively, and the respective kinase activities of the receptor complexes are denoted a_1 and a_2. The membrane cluster senses an external ligand concentration L. As in [15], we allow for a degree of communication between the two clusters through a signal that is a function of the membrane cluster

activity, a_1. This signal scales the external ligand signal L to form the signal $\tilde{L}$ that is sensed by the cytoplasmic cluster.

If, as in the *E. coli* model in [4], we assume that the chemotaxis protein phosphorylation dynamics are fast compared to the methylation dynamics, we can represent the *R. sphaeroides* chemotaxis model in [15] as

$$\begin{aligned}\dot{m}_1&=K_3(1-a_1)-K_2a_1[B_1(a_1)+B_2(a_2)],\ a_1=\frac{m_1}{K_1+L}\\ \dot{m}_2&=K_3(1-a_2)-K_2a_2[B_2(a_2)],\ a_2=\frac{m_2}{K_1+\tilde{L}},\ \tilde{L}=\frac{L}{a_1}\end{aligned} \tag{21}$$

It can be shown that a_1 is bounded by 1, and therefore if $L \gg K_1$ then $\tilde{L} \gg K_1$, in which case $a_1 \approx \frac{m_1}{L}$ and $a_2 \approx \frac{m_2}{\tilde{L}}$ which allows us to approximate (21) by

$$\begin{aligned}&\begin{bmatrix}\dot{m}_1\\ \dot{m}_2\end{bmatrix}=\begin{bmatrix}K_3(1-a_1)-K_2a_1[B_1(a_1)+B_2(a_2)]\\ K_3(1-a_2)-K_2a_2[B_2(a_2)]\end{bmatrix}\\ &a_1=\frac{m_1}{L_1},\ a_2=\frac{m_2}{\tilde{L}},\ \tilde{L}=\frac{L_1}{a_1}\end{aligned} \tag{22}$$

We wish to study the activity responses $a_1(t), a_2(t)$ of this system when it is subject to a ligand input signal $L(t) = L_1(t)$ and to positive scalings of this signal, given by $L(t) = L_2(t) = pL_1(t)$, $p > 0$. By letting $\rho(m_1, m_1) = \frac{1}{p}\begin{bmatrix} m_1 & m_2 \end{bmatrix}^T$ and $\lambda(m_1, m_2) = \frac{1}{p}$, we find that (22) satisfies the conditions of Proposition 1 and that a scaling by $p > 0$ of the input L that is applied to (22) results in a time scaling of the outputs a_1, a_2 of this system by p^{-1}. This is illustrated for the output a_1 in Figure 7.

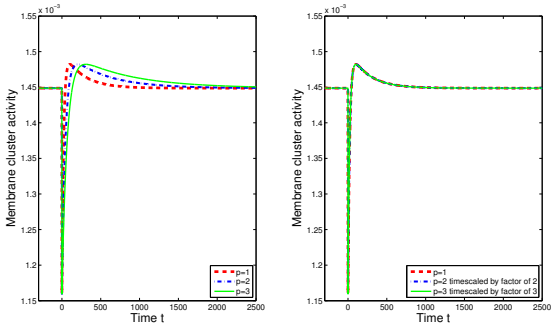

Fig. 7. Left: Simulated outputs $a_1(t)$ of the model (22) subject to inputs $pL_1(t)$, $p = 1, 2, 3$. The signal $L(t)$ is a 25% step at time $t = 0$, where $L(0_-) = 750$. Right: Simulated outputs time scaled by p. Model parameters: $K_1 = 20, K_1 = 33.75, K_3 = 0.0612, B_1(a_1) = 1, B_2(a_2) = 0.2$.

V. Discussion

We have presented conditions under which transformations of step inputs applied to adapting systems cause a time scaling of their output responses. These results extend earlier results that give conditions for fold change detection. We have shown that the conditions for systems to display time scaling are less restrictive than those required for exact FCD. Furthermore, we have shown that by quantifying the degree of time scaling, we can measure the extent of the system response's deviation from FCD.

Appendix

We can assume that receptors are either bound or unbound to ligand, and either active or inactive. The binding reaction between inactive receptors (concentration $[I]$) and ligands (concentration $[L]$), which has dissociation constant K_I, can be represented as $[I] + [L] \leftrightarrow [IL]$ so that in steady state $[IL]K_I = [I][L]$. Similarly, the reaction between active receptors (concentration $[A]$) and ligands, which has dissociation constant K_A, is $[A] + [L] \leftrightarrow [AL]$ so that in steady state $[AL]K_A = [A][L]$. The average receptor activity level a can be approximated as

$$a = \frac{[AL]+[A]}{[AL]+[A]+[IL]+[I]} = \frac{1}{1+\frac{[I]}{[A]}\left[\frac{1+\frac{L}{K_I}}{1+\frac{L}{K_A}}\right]} \tag{23}$$

When the receptors form clusters of size N, the above derivation can be extended to arrive at the model of the activity given by $a = \frac{1}{1+\frac{[I]}{[A]}\left[\frac{1+\frac{L}{K_I}}{1+\frac{L}{K_A}}\right]^N}$. The quantity $\frac{[A]}{[I]}$, which is the ratio of active to inactive receptors when $L = 0$, increases with the average receptor methylation level m and can hence be modeled as a strictly increasing function $h(m)$.

References

[1] Yi TM, Huang Y, Simon MI, Doyle J 2000. Robust perfect adaptation in bacterial chemotaxis through integral feedback control. *Proc Natl Acad Sci USA* **97**(9), 46494653.

[2] Barkai N, Leibler S 1997. Robustness in simple biochemical networks. *Nature* **387**, 913-917.

[3] Shoval O, Goentoro L, Hart Y, Mayo A, Sontag E, and Alon U 2010. Fold-change detection and scalar symmetry of sensory input fields. *Proc Natl Acad Sci USA* **107**(36), 1599516000.

[4] Tu Y, Shimizu TS, Berg HC 2008. Modeling the chemotactic response of *Escherichia coli* to time-varying stimuli. *Proc Natl Acad Sci USA* **105**(39), 1485514860.

[5] Emonet T, Cluzel P, 2008. Relationship between cellular response and behavioral variability in bacterial chemotaxis. *Proc Natl Acad Sci USA*, **105**:3304-3309.

[6] Porter SL, Wadhams GH, Armitage JP 2011 Signal processing in complex chemotaxis pathways. *Nat Rev Microbiol* **9**(3), 153-65.

[7] Rao CV, Kirby JR, Arkin AP 2004. Design and Diversity in Bacterial Chemotaxis: A Comparative Study in *Escherichia coli* and *Bacillus subtilis*. *PLoS Biol* **2**(2): e49. doi:10.1371/journal.pbio.0020049

[8] Mesibov R, Ordal G, Adler J 1973. The range of attractant concentrations for bacterial chemotaxis and the threshold and size of response over this range. *J Gen Physiol* **62**:203 223.

[9] Monod J, Wyman J, Changeux JP 1965. On the nature of allosteric transitions: A plausible model. *J Mol Biol* **12**, 88118.

[10] Keymer JE, Endres RG, Skoge M, Meir Y, Wingreen NS 2006. Chemosensing in Escherichia coli: Two regimes of two-state receptors. *Proc Natl Acad Sci USA* **103**(6), 17861791.

[11] Shimizu TS, Tu Y, Berg HC, 2010. A modular gradient-sensing network for chemotaxis in *Escherichia coli* revealed by responses to time-varying stimuli. *Mol. Syst. Biol.* **6**:382

[12] Morton-Firth CJ, Shimizu TS, Bray D 1999. A Free-energy-based Stochastic Simulation of the Tar Receptor Complex. *J Mol Biol* **286**, 1059-1074.

[13] Lazova MD, Ahmed T, Bellomo D, Stocker R, Shimizu TS 2011. Response rescaling in bacterial chemotaxis. *Proc Natl Acad Sci USA* **108**(33), 1387013875.

[14] Shoval O, Alon U, and Sontag ED 2011. Symmetry invariance for adapting biological systems. *SIAM J Appl Dyn Syst* **10**, 857-886.

[15] Hamadeh A, Roberts M, August E, McSharry P, Maini P, Armitage J, Papachristodoulou A 2011. Feedback control architecture and the bacterial chemotaxis network. *PLoS Comp Biol* **7**(5), e1001130.